

# On the Generalizability of Foundation Models for Crop Type Mapping

Yi-Chia Chang<sup>1</sup>, Adam J. Stewart<sup>2</sup>, Favyen Bastani<sup>3</sup>, Piper Wolters<sup>3</sup>,  
Shreya Kannan<sup>1</sup>, George R. Huber<sup>1</sup>, Jingtong Wang<sup>1</sup>, Arindam Banerjee<sup>1</sup>

<sup>1</sup>University of Illinois Urbana-Champaign,

<sup>2</sup>Technical University of Munich,

<sup>3</sup>Allen Institute for AI

## Abstract

Foundation models pre-trained using self-supervised and weakly-supervised learning have shown powerful transfer learning capabilities on various downstream tasks, including language understanding, text generation, and image recognition. Recently, the Earth observation (EO) field has produced several foundation models pre-trained directly on multispectral satellite imagery (e.g., Sentinel-2) for applications like precision agriculture, wildfire and drought monitoring, and natural disaster response. However, few studies have investigated the ability of these models to generalize to new geographic locations, and potential concerns of geospatial bias—models trained on data-rich developed countries not transferring well to data-scarce developing countries—remain. We investigate the ability of popular EO foundation models to transfer to new geographic regions in the agricultural domain, where differences in farming practices and class imbalance make transfer learning particularly challenging. We first select six crop classification datasets across five continents, normalizing for dataset size and harmonizing classes to focus on four major cereal grains: maize, soybean, rice, and wheat. We then compare three popular foundation models, pre-trained on SSL4EO-S12, SatlasPretrain, and ImageNet, using in-distribution (ID) and out-of-distribution (OOD) evaluation. Experiments show that pre-trained weights designed explicitly for Sentinel-2, such as SSL4EO-S12, outperform general pre-trained weights like ImageNet. Furthermore, the benefits of pre-training on OOD data are the most significant when only 10–100 ID training samples are used. Transfer learning and pre-training with OOD and limited ID data show promising applications, as many developing regions have scarce crop type labels. All harmonized datasets and experimental code are open-source and available for download.

## 1 Introduction

Crop type maps have many critical downstream uses in food security and conservation, including crop yield prediction (Khaki and Wang, 2019; Doraiswamy et al., 2003; Van Klompenburg et al., 2020; Fan et al., 2022), understanding interactions between wildlife and crop fields (Gross et al., 2018; Pywell et al., 2015), and regional crop damage assessment (Silleos et al., 2002; Rahman and Di, 2020).

However, the availability and accuracy of crop type maps varies greatly across regions: the US and EU maintain large-scale, regularly updated maps with 80+% accuracy (Verhegghen et al., 2021; Luman and Tweddale, 2008), but crop type maps of most other regions are sporadically updated and much lower in accuracy, due to weaker crop type self-reporting policies, less government resources, and a greater prevalence of smallholder farming that is more difficult to map. Even sparse high-accuracy crop type labels are rare in these regions. Thus, while numerous methods have been proposed to map crop types through remote sensing (Prins and Van Niekerk, 2021; Adrian et al., 2021; Tang et al., 2024; Yuan et al., 2023), these have

seldom been deployed globally, since high-quality training data does not exist for most of the world.

Nevertheless, we argue that recent remote sensing foundation models like SSL4EO-S12 (Wang et al., 2023) and SatlasPretrain (Bastani et al., 2022), that are trained on globally available image sources such as Landsat OLI-TIRS, Sentinel-1, and Sentinel-2, present a key opportunity for increasing the accuracy of global crop type mapping by improving the ability for models trained on downstream tasks to generalize across regions. However, transfer learning for crop type mapping in concert with such foundation models has not been studied at scale, in part because of the lack of a harmonized dataset of global crop type labels.

In this paper, we first present a harmonized global crop type mapping dataset that incorporates six regional datasets across five continents. We identify the available data source(s) with the highest label quality in each continent and pair their crop type labels with a uniform collection of cloud-free Sentinel-2 images captured during the peak of the growing season in each region. We focus on four major cereal grains and harmonize the class labels of each dataset around these categories. We integrate this dataset into TorchGeo (Stewart et al., 2022), a popular library for deep learning with remote sensing data, to make it easy for other researchers to reproduce our work and perform their own experiments. Moreover, we then perform a detailed study on the effectiveness of transfer learning for crop type mapping using remote sensing foundation models.

In summary, this paper’s contributions include:

- We harmonize six existing crop type datasets from five continents.
- We perform a range of benchmark experiments to study the efficacy of remote sensing foundation models and transfer learning.
- We evaluate the benefits of pre-training with out-of-distribution and in-distribution data.
- All datasets, data modules, and experiment training scripts have been integrated into TorchGeo.

## 2 Related Work

### 2.1 Crop Type Datasets

Several remote sensing datasets for crop type mapping have been developed. However, most existing datasets are limited to individual countries or regions: for example, PASTIS Garnot et al. (2022) is limited to southern France, and AgriFieldNet Radiant Earth Foundation and IDinsight (2022) is limited to northern India. This limited geographic diversity makes it difficult to study the effectiveness of transfer learning across climatic regions and political borders. While it is possible to train on one dataset and test on a dataset from a different region, each dataset provides a distinct set of class labels that is challenging to harmonize.

At the same time, several large-scale country-level crop type maps are available that are not geared towards remote sensing, including the Croplands Data Layer (CDL) in the US and various self-declared crop reporting datasets in the EU. While these maps are much larger in scale than existing remote sensing datasets, and comparable in accuracy, using them for training remote sensing models requires first acquiring aligned satellite images. This requires some engineering effort, and as a result these maps are underutilized for machine learning. Our harmonized dataset includes Sentinel-2 images aligned with several such maps that we downloaded and re-projected, eliminating this barrier.

### 2.2 Studies on Remote Sensing for Crop Type Mapping

A few works have studied the effectiveness of remote sensing methods for mapping crop types from satellite imagery. CropHarvest (Tseng et al., 2021) is a global dataset that pairs single-pixel satellite image time

Table 1: A list of the datasets used in this study. All datasets are manually vetted and harmonized for global model training. Number of classes includes “other” but excludes “nodata”. Resolution is measured in meters per pixel. Labels collected by ground survey or self-declaration are considered to be close to 100% accurate, while ML-labeled datasets are listed with their reported overall accuracy on the principal crop classes. Datasets are listed in order of decreasing number of patches.

Dataset	Region	# Patches	# Classes	Res.	Accuracy	License
CDL	USA	770,954	134	30	84.1%	CC0-1.0
NCCM	China	402,000	4	10	87%	CC-BY-4.0
SAS	S. America	326,535	2	30	96%	Unknown
EuroCrops	Europe	259,191	331	-	Self-declared	CC-BY-SA-4.0
SACT	S. Africa	5,516	9	10	Ground survey	CC-BY-4.0
AgriFieldNet	India	1,217	13	10	Ground survey	CC-BY-4.0
Harmonized	Global	1,765,413	5	10	87.47%	CC-BY-SA-4.0

series with crop type labels. The authors find that training on the entire dataset and then fine-tuning on individual regions improves performance compared to training on the regions alone; however, they do not make use of remote sensing foundation models to improve generalizability, and do not consider transferring from one region to another. Furthermore, the focus on individual pixels rather than image patches makes it impossible to apply models like CNNs or ViTs that leverage spatial context to improve prediction accuracy.

### 2.3 Remote Sensing Foundation Models

Several foundation models for processing satellite and aerial imagery have recently been proposed (Manas et al., 2021; Mall et al., 2023a,b). SSL4EO-S12 Wang et al. (2023) applies MoCo v2 Chen et al. (2020) on three million patches of Sentinel-1 and Sentinel-2 images from diverse geographies. SatlasPretrain Bastani et al. (2022) employs supervised learning on twenty million patches of Sentinel-2 and NAIP images, using globally available sources of vector geospatial data like OpenStreetMap as labels. Both foundation models show substantial gains when fine-tuned on downstream applications. Thus, we believe that these remote sensing foundation models have the potential to improve the transferability of crop type classification across different regions.

## 3 Global Harmonized Crop Type Dataset

Dozens of existing crop type classification datasets exist in the literature, with varying label quality and crop type categories. While a few small-scale datasets are manually labeled by experts, the majority of large-scale datasets are generated by machine learning models and must first be vetted by experts before they can reliably be used for further model training. In order to facilitate the training of global crop type classification models, we manually inspected and verified the validity of all publicly available crop type classification datasets and selected six datasets from five continents noteworthy for their size and label accuracy. Table 1 lists all six datasets, as well as statistics about the dataset size and estimated accuracy levels published by their original authors.

Since each dataset includes a different number of crop classes with differing levels of granularity, we first harmonize all mask labels to six classes: 0: no data (unknown), 1: maize (corn), 2: soybean, 3: rice, 4: wheat, and 5: other (known). The class harmonization details can be found in the Appendix.

Maize, soybean, rice, and wheat are chosen as the four major cereal grains in our study. These four crop types represent the four most valuable crops worldwide, making up the vast majority of all global ce-

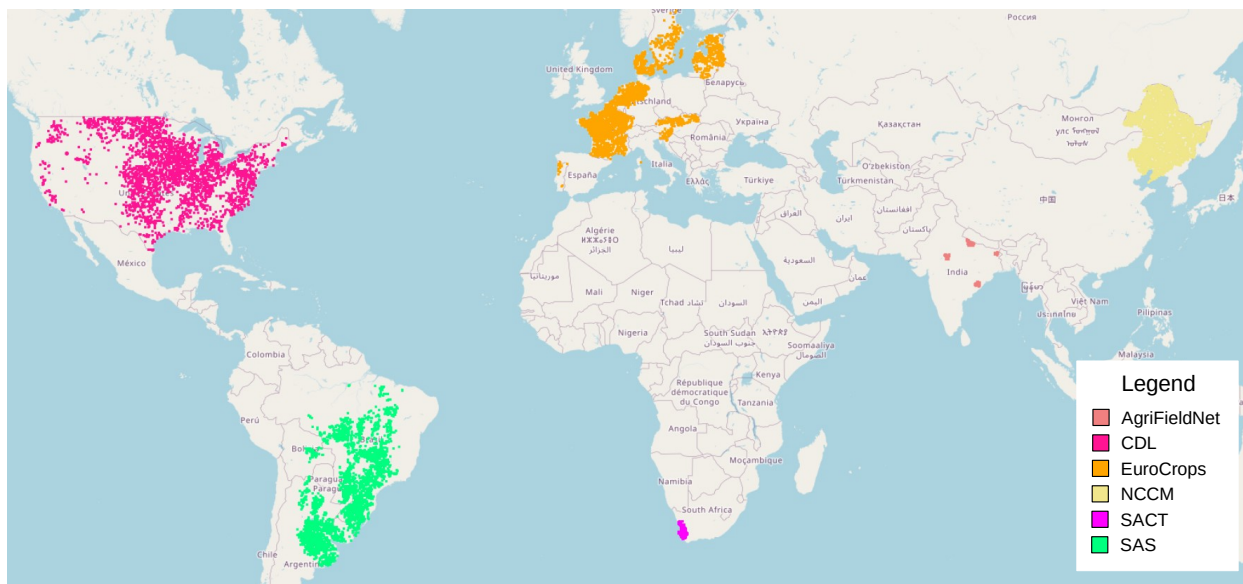


Figure 1: Locations covered by each of the six crop type datasets that make up our global harmonized dataset. The dataset covers five continents: Asia, Africa, Europe, North America, and South America. The details of the datasets are shown in Table 1.

real production (grasses cultivated for their edible grains) and roughly half of agricultural lands worldwide Martin et al. (2019). They are also prevalent in all of the datasets we chose, albeit with very different frequencies. We also reserve classes for “other”, including both other forms of agriculture and non-agricultural land use, and “nodata”, where the land cover type is unknown and may or may not include one of our four crop types of interest. All nodata pixels are ignored in this study when computing metrics so as to avoid unfairly penalizing the model. We exclude image patches in our study without any fields (for vector datasets) or less than 32 pixels (for raster datasets) belonging to these four crop types so as to avoid images that are almost entirely “other” or “nodata”.

After class harmonization, we chip each dataset into  $256 \times 256$  px patches. As the majority of these datasets are published as raster and vector mask layers without any corresponding imagery, we download our own Sentinel-2 imagery for each labeled region from Google Cloud<sup>1</sup>. For each mask, we download a cloud-free Sentinel-2 L1C image patch for the same location during the peak of the growing season (depending on latitude) during the year the mask was acquired. This is also done for the few datasets that do come with imagery so as to ensure that all Sentinel-2 spectral bands are present in the image. All images and masks are then warped to a Web Mercator projection at 10 m/px resolution.

All preprocessed datasets used in this study are available for download from Hugging Face, and data loaders are provided through the TorchGeo (Stewart et al., 2022) library. This not only allows for easy reproducibility, but also for future experimentation and benchmarking. Figure 1 displays the geographic coverage of the combined harmonized dataset. Additional dataset-specific details can be found below.

### 3.1 Cropland Data Layer (CDL)

The Cropland Data Layer (CDL) (USDA NASS, 2024) is an annual crop classification product released by the National Agricultural Statistics Service (NASS) of the United States Department of Agriculture (USDA) spanning the entire contiguous United States (CONUS) from 1997 to present. It has a spatial resolution of 30 m/px, and is generated by decision tree classifiers trained on time-series imagery from the Landsat 8

<sup>1</sup><https://cloud.google.com/storage/docs/public-datasets/sentinel-2>

and 9 OLI/TRS and Sentinel-2 satellites collected throughout the growing season.

Note that all classes denoting double cropping (the practice of planting different crops in the spring and fall) are explicitly left out of the dataset as it is not possible to know which crop was planted at the time of our image. These pixels make up a very small portion of the dataset anyway. The 2023 CDL product is downloaded and resampled to 10 m resolution, and Sentinel-2 imagery from 2023-07-01 to 2023-08-01 is gathered for this portion of the harmonized dataset.

### **3.2 Northeast China Crop Type Maps (NCCM)**

The Northeast China Crop Type Maps (NCCM) (You et al., 2021) dataset consists of annual crop maps of major crop types in northeast China. Labels are available for 2017–2019 and are created using a combined hierarchical mapping strategy, agro-climate zone-specific random forest classifiers, time-series Sentinel-2 imagery, and various other hand-crafted feature extractors. Our study used the most recent and highest-accuracy 2019 crop map. We downloaded the corresponding Sentinel-2 imagery from July 2019.

### **3.3 South America Soybean (SAS)**

South America Soybean (SAS) (Song et al., 2021) is a binary classification map created for South America to map the expansion of soybean plantations and deforestation between 2000 and 2019. Landsat and MODIS satellite imagery were used to train an ensemble of decision tree classifiers to make predictions at 30 m resolution. In our study, we resample these masks to 10 m resolution.

It is worth noting that since SAS is a binary classification dataset, it is likely that the “other” class we used actually contains maize, rice, and/or wheat. Unfortunately, we were unable to find any multiclass crop classification datasets for South America. The most recent 2021 version of the dataset was used, along with Sentinel-2 imagery downloaded from July 2021.

### **3.4 EuroCrops**

EuroCrops (Schneider et al., 2023) is a collection of publicly available crop classification datasets from across Europe. All labels are stored in vector files with polygons for each field and come from self-reported agricultural databases from the European Union. All data is rasterized and harmonized from 275 Hierarchical Crop and Agriculture Taxonomy (HCAAT) codes to the classes we consider in our paper. EuroCrops version 9 was used in this study. The images were downloaded from the corresponding years of each country (2018–2021) during July.

### **3.5 South Africa Crop Type Competition (SACT)**

The South Africa Crop Type (SACT) (Western Cape Department of Agriculture and Radiant Earth Foundation, 2021) competition dataset was created for the Radiant Earth Spot the Crop Challenge and includes time-series Sentinel-1 SAR, Sentinel-2 MSI, and masks for 9 crop classes. The data was collected by aerial and vehicle surveys by the Western Cape Department of Agriculture. Only the training set is used in this study, as the testing set was never publicly released. All time-series imagery was replaced with our own static Sentinel-2 imagery from February 2017 to May 2017 (Southern Hemisphere summer) for fair comparison across datasets.

### **3.6 AgriFieldNet**

The AgriFieldNet India Competition (Radiant Earth Foundation and IDinsight, 2022) dataset includes satellite imagery from Sentinel-2 cloud-free composites (single snapshot) and crop type labels that were collected

Table 2: Overall accuracies for ID experiments. SSL4EO-S12 constantly outperforms the other two pre-trained weights in all regions. The experiments are implemented three times with seeds.

Pre-trained weights	CDL	NCCM	EuroCrops	AgriFieldNet	SAS	SACT
SSL4EO-S12	<b>87.37 ± 0.17</b>	<b>88.75 ± 0.14</b>	<b>82.23 ± 0.51</b>	<b>60.23 ± 1.76</b>	<b>83.34 ± 0.38</b>	<b>82.72 ± 0.54</b>
SatlasPretrain	77.87 ± 1.85	80.56 ± 0.38	77.71 ± 1.36	52.79 ± 0.14	75.35 ± 0.34	78.20 ± 0.00
ImageNet	78.77 ± 1.31	82.71 ± 0.33	78.02 ± 0.38	52.20 ± 2.61	80.05 ± 0.20	79.10 ± 0.17

by ground survey in India. The dataset contains 7,081 fields across 4 states in northern India, which have been split into training and test sets (5,551 fields in the train and 1,530 fields in the test). Only the training set is used in this study, as the testing set was never publicly released. Satellite imagery and labels are tiled into  $256 \times 256$  chips adding up to 1,217 tiles. All original images are replaced by our own consistent Sentinel-2 imagery downloaded from June 2021 to August 2021. In the experiments, we use the training samples to create a train-test split.

## 4 Experimental Setup

Below, we describe the experimental setup for all experiments performed in this study. Throughout all experiments, we freeze the ResNet-50 encoder and fine-tuned a U-Net decoder. We follow the same normalization methods as SSL4EO-S12, SatlasPretrain, and ImageNet for the satellite imagery input. All reported metrics use overall accuracy (OA). Data augmentation is implemented to improve model performance during OOD +  $k$  ID and  $k$  ID training, including random horizontal and vertical flip and random resized crop data. We use the default learning rate  $1e-3$  and AdamW optimizer (Loshchilov and Hutter, 2019). The maximum epochs is 100, and the batch size is 128. All experiments are performed in 8 NVIDIA RTX A6000 GPUs with 48 GB of memory. The total GPU consumption for all experiments is approximately 150 GPU hours.

### 4.1 Pre-trained Weights Selection

In the first experiment, we explore various pre-trained weights to find one that performs best on all regions. We fine-tune a U-Net decoder using frozen ResNet-50 backbones pre-trained on ImageNet (He et al., 2016), SSL4EO-S12, and SatlasPretrain. SSL4EO-S12 and SatlasPretrain are state-of-the-art foundation models pre-trained directly on multispectral Sentinel-2 imagery, while ImageNet was chosen as a baseline due to its widespread use in machine learning research. All models are evaluated on the full dataset sizes reported in Table 1, with a separate 80-10-10 train-val-test split for each geographic region. Validation splits are used to determine the optimal set of hyperparameters, and the test set is used to decide the best performing set of pre-trained weights for use in all subsequent experiments.

### 4.2 In-Domain (ID) Evaluation

Next, we use the best-performant pre-trained weights (SSL4EO-S12) to explore the effects of the number of ID training data (see the last three columns of Table 3). In this experiment and all subsequent experiments, we select a subset of 1,000 images to fairly compare all datasets. 1,000 is chosen to match the smallest dataset, AgriFieldNet. Each dataset uses a 90-10 train-test split. We then investigate how performance changes based on different numbers of ID data. The numbers of training data usage range from 10 to 900. The various training data usage enables us to understand the effects of increasing training data.

Table 3: Overall accuracies on each dataset when trained on ID and OOD +  $k$  ID samples. Increasing ID data improves model performance in most regions. Pre-training OOD with ID data is beneficial with limited ID data.

Dataset	OOD	OOD + 10 ID	OOD + 100 ID	OOD + 900 ID	10 ID	100 ID	900 ID
CDL	71.31	77.74	79.20	<b>85.59</b>	69.78	77.53	<b>85.05</b>
NCCM	68.14	75.12	84.79	<b>90.06</b>	72.63	85.89	<b>90.12</b>
SAS	59.33	66.92	78.86	<b>86.25</b>	66.50	78.34	<b>85.01</b>
EuroCrops	61.52	67.72	73.56	<b>80.58</b>	68.19	75.17	<b>82.05</b>
SACT	65.38	68.09	74.35	<b>79.31</b>	68.83	73.47	<b>80.37</b>
AgriFieldNet	<b>49.87</b>	46.53	41.95	29.36	29.04	40.46	<b>51.90</b>

### 4.3 Few-shot Learning and Transferability

To assess how well foundation models can adapt to shifts in data distribution, we divide the regions into in-distribution (ID) and out-of-distribution (OOD) zones, following a similar approach to Sachdeva et al. (2024). Specifically, we train models using SSL4EO-S12 pre-trained weights on 5 regions (OOD) and test on 1 region (ID) for the few-shot learning (see the first four columns of Table 3). The models are trained on OOD zones and  $k$  number of samples from ID zones, then tested on ID zones. For the fair comparison, 100 test data are exclusively selected for evaluating model performance. All models trained with  $k$  ID and OOD +  $k$  ID are evaluated with the same exclusive test data.

## 5 Benchmark Results

### 5.1 SSL4EO-S12 Outperforms in the ID Settings

Table 2 shows that SSL4EO-S12 has the best performance in all regions. Although SatlasPretrain has state-of-the-art performances in various downstream tasks, such as building and road detections, it shows mixed performances with ImageNet in the crop type mapping task. On the other hand, SSL4EO-S12 steadily outperforms by 4 to 9%, showing that pre-trained weights designed for Sentinel-2 perform better than the multimodal and general pre-trained weights when using solely Sentinel-2 imagery.

### 5.2 Pre-training on Out-of-Distribution Is Beneficial with Limited In-Distribution Data

The advantages of pre-training on OOD data are particularly profound in scenarios with limited labeled training data. Table 3 shows the results of  $k$  ID and OOD +  $k$  ID test results. With only 10 ID training data points, pre-training on OOD can outperform models trained solely with ID data. For example, without any CDL training samples, the model trained with the other 5 OOD regions can reach 71.31% accuracy, already better than using 10 ID training data in CDL. By adding 10 ID data with OOD, the performance can further increase to 77.74%. Compared to solely training with 10 ID data, the model improves 7.9% from 69.78%. With the increase of ID data to 100, pre-training on OOD slightly improves the performance from 0.8–1.6% for CDL, AgriFieldNet, SAS, and SACT compared to using only 100 ID data. This finding is promising for geospatial transferability, as many developing regions have scarce crop type labels.

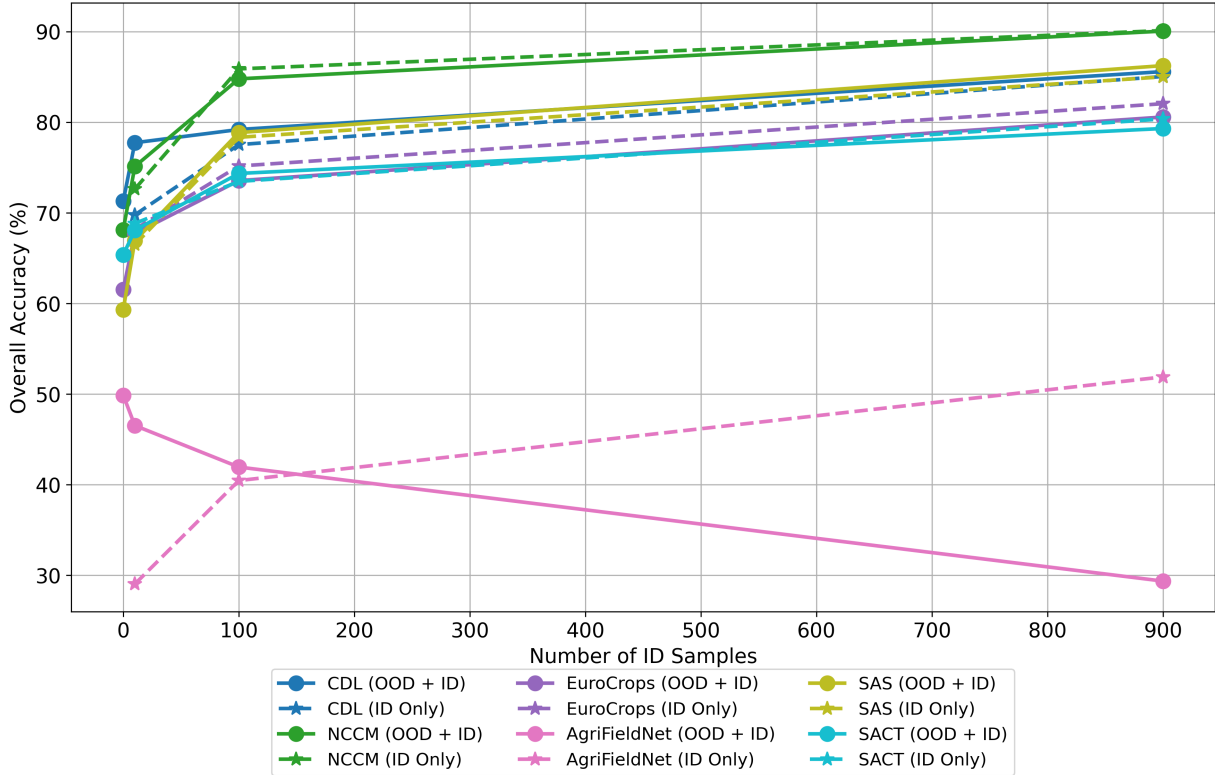


Figure 2: The overall accuracy comparison between OOD +  $k$  ID and  $k$  ID as  $k$  changes. The results are computed from Table 3 showing the cross-over of OOD +  $k$  ID and  $k$  ID settings. Most regions increase overall accuracy as the number of ID data increases and have close performance with OOD + 900 ID and 900 ID. The cross-over happens mostly between 100 and 900 ID.

### 5.3 More ID Data Should Be Prioritized

Figure 2 shows that more ID data generally improve the model performance in both OOD + ID and ID settings. As the number of ID training data increases, the advantages of OOD pre-training diminish. For instance, NCCM’s model with OOD + 10 ID has a 2.49% accuracy increase compared to the model solely trained with 10 ID. As the ID data increases to 100 and 900, the model performance changes are not significant. When using the full ID training samples, the highest test accuracy occurs in both OOD + ID and ID settings. It highlights the importance of prioritizing ID data to train models for target areas when more ID training data is available. Overall, the advantages of pre-training on OOD are the most significant when small amounts of ID training samples are used, which will be beneficial for data-scarce regions. Future research can explore pre-training on different combinations of high-accuracy datasets, such as CDL, NCCM, and EuroCrops.

### 5.4 Region-wise Comparison

Despite being trained on ML-generated labels, CDL and NCCM show higher accuracy than all other datasets. The phenomenon could be due to the fact that the data generated by ML models makes it easier for other ML models to reproduce similar data even if there are errors. Conversely, despite AgriFieldNet containing manually-labeled ground truth data collected during a ground survey and the same number of image patches as all other datasets, it actually has the lowest accuracy. As seen in the class distribution table (see



the appendix) in the supplementary material, this wide range of overall accuracy is likely due to class imbalance, with labeled fields in AgriFieldNet making up a much smaller portion of the dataset than “other” pixels. In data-scarce regions, such as India, South Africa, and South America, models trained on a combination of OOD and 100 ID data perform slightly better than solely 100 ID data. For AgriFieldNet, pre-training on OOD provides a strong foundation.

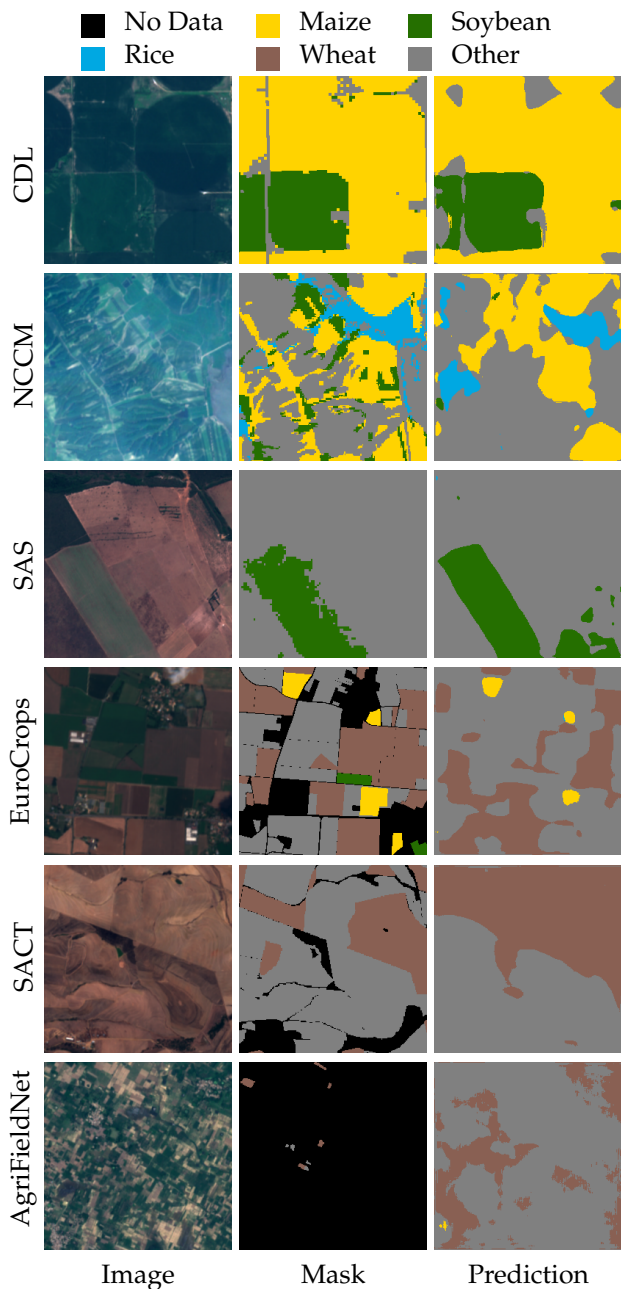


Figure 3: Visualization of example input Sentinel-2 images, ground truth masks, and model predictions for all datasets. Overall results are promising, with the ID models capturing the general class distribution and correctly identifying most fields.

Figure 2 and other metrics as  $k$  changes (see the appendix) illustrate the effect of few-shot OOD training, with class-wise averaging and overall averaging for accuracy, precision, recall, and F1 score. We note two

interesting behaviors discovered during these experiments. First, while overall performance metrics tend to show a slight improvement as  $k$  (the number of OOD training examples) increases, class-wise averaged performance metrics show a much greater increase. This demonstrates that OOD training is critical for classes that are less common in ID settings. Second, AgriFieldNet greatly deviates from the trend seen in other datasets, suggesting that the extreme class imbalance present in the dataset actually hurts model performance, resulting in a model that regularly predicts “other” since it is the most common class.

The results in Figure 3 are visualized using weights of OOD + 900 ID for SAS, and 900 ID for CDL, NCCM, EuroCrops, SACT, and AgriFieldNet. The most obvious visual difference between mask and prediction is the loss of fine-scale features like roads, as seen in prior works on CDL crop classification using foundation models Stewart et al. (2024). This is especially evident in the second row of the figure, where intercropping (the practice of planting rows of different crops in close proximity) is seen for maize and soybean. In the CDL predictions, it is also possible to see that the model frequently predicts wheat near the boundary of fields, possibly due to the similar resemblance of weeds.

## 6 Conclusion

In this work, we present the first global semantic segmentation dataset for crop classification, created by harmonizing six crop classification datasets from five continents. We investigate the ability of various pre-trained foundation models to perform crop classification in ID, OOD, and OOD +  $k$  ID sample settings. This work provides interesting findings for the future challenge of global crop classification and elucidates many of the limitations of existing datasets and modeling strategies. Larger datasets are needed, especially for regions like India and South Africa where large datasets are scarce. However, dataset size is not the only important factor, with class imbalance plaguing all datasets used in this study. In order to correctly predict uncommon classes with higher precision, especially when models move from the four most important cereal grains to hundreds of agricultural classes, the issue of class imbalance will need to be addressed, either through weighted dataset sampling or weighted loss functions.

**Acknowledgement.** The work was supported in part by the National Science Foundation (NSF) through awards IIS 21-31335, OAC 21-30835, DBI 20-21898, as well as a C3.ai research award. This work made use of the Illinois Campus Cluster, a computing resource that is operated by the Illinois Campus Cluster Program (ICCP) in conjunction with the National Center for Supercomputing Applications (NCSA) and which is supported by funds from the University of Illinois at Urbana-Champaign. The work was supported in part by the Taiwan-UIUC Fellowship.

## References

- Adrian, J., Sagan, V., and Maimaitijiang, M. (2021). Sentinel sar-optical fusion for crop type mapping using deep learning and google earth engine. *ISPRS Journal of Photogrammetry and Remote Sensing*, 175:215–235.
- Bastani, F., Wolters, P., Gupta, R., Ferdinando, J., and Kembhavi, A. (2022). Satlaspretrain: A large-scale dataset for remote sensing image understanding. *2023 IEEE/CVF International Conference on Computer Vision (ICCV)*, pages 16726–16736.
- Chen, X., Fan, H., Girshick, R., and He, K. (2020). Improved baselines with momentum contrastive learning. *arXiv preprint arXiv:2003.04297*.
- Doraiswamy, P. C., Moulin, S., Cook, P. W., and Stern, A. (2003). Crop yield assessment from remote sensing. *Photogrammetric Engineering & Remote Sensing*, 69(6):665–674.

- Fan, J., Bai, J., Li, Z., Ortiz-Bobea, A., and Gomes, C. P. (2022). A gnn-rnn approach for harnessing geospatial and temporal information: Application to crop yield prediction. *Proceedings of the AAAI Conference on Artificial Intelligence*, 36(11):11873–11881.
- Garnot, V. S. F., Landrieu, L., and Chehata, N. (2022). Multi-modal temporal attention models for crop mapping from satellite time series. *ISPRS Journal of Photogrammetry and Remote Sensing*, 187:294–305.
- Gross, E. M., Lahkar, B. P., Subedi, N., Nyirenda, V. R., Lichtenfeld, L. L., and Jakoby, O. (2018). Seasonality, crop type and crop phenology influence crop damage by wildlife herbivores in africa and asia. *Biodiversity and Conservation*, 27:2029–2050.
- He, K., Zhang, X., Ren, S., and Sun, J. (2016). Deep residual learning for image recognition. In *Proceedings of the IEEE Conference on Computer Vision and Pattern Recognition (CVPR)*.
- Khaki, S. and Wang, L. (2019). Crop yield prediction using deep neural networks. *Frontiers in plant science*, 10:452963.
- Loshchilov, I. and Hutter, F. (2019). Decoupled weight decay regularization.
- Luman, D. and Tweddale, T. (2008). Assessment and potential of the 2007 usda-nass cropland data layer for statewide annual land cover applications. *Technical Report INHS 2008 (49)*.
- Mall, U., Hariharan, B., and Bala, K. (2023a). Change-aware sampling and contrastive learning for satellite images. In *Proceedings of the IEEE/CVF Conference on Computer Vision and Pattern Recognition*, pages 5261–5270.
- Mall, U., Phoo, C. P., Liu, M. K., Vondrick, C., Hariharan, B., and Bala, K. (2023b). Remote sensing vision-language foundation models without annotations via ground remote alignment. In *The Twelfth International Conference on Learning Representations*.
- Manas, O., Lacoste, A., Giró-i Nieto, X., Vazquez, D., and Rodriguez, P. (2021). Seasonal contrast: Unsupervised pre-training from uncurated remote sensing data. In *Proceedings of the IEEE/CVF International Conference on Computer Vision*, pages 9414–9423.
- Martin, A. R., Cadotte, M. W., Isaac, M. E., Milla, R., Vile, D., and Violle, C. (2019). Regional and global shifts in crop diversity through the anthropocene. *PLoS One*, 14(2):e0209788.
- Prins, A. J. and Van Niekerk, A. (2021). Crop type mapping using lidar, sentinel-2 and aerial imagery with machine learning algorithms. *Geo-Spatial Information Science*, 24(2):215–227.
- Pywell, R. F., Heard, M. S., Woodcock, B. A., Hinsley, S., Ridding, L., Nowakowski, M., and Bullock, J. M. (2015). Wildlife-friendly farming increases crop yield: evidence for ecological intensification. *Proceedings of the Royal Society B: Biological Sciences*, 282(1816):20151740.
- Radiant Earth Foundation and IDinsight (2022). Agrifieldnet competition dataset. Radiant MLHub. Version 1.0.
- Rahman, M. S. and Di, L. (2020). A systematic review on case studies of remote-sensing-based flood crop loss assessment. *Agriculture*, 10(4):131.
- Sachdeva, S., Lopez, I., Biradar, C., and Lobell, D. (2024). A distribution shift benchmark for smallholder agroforestry: Do foundation models improve geographic generalization? *The Twelfth International Conference on Learning Representations 2024 Machine Learning for Remote Sensing (MLARS) Workshop*.
- Schneider, M., Schelte, T., Schmitz, F., and Körner, M. (2023). EuroCrops: The largest harmonized open crop dataset across the European Union. *Scientific Data*, 10(1):612.

- Silleos, N., Perakis, K., and Petsanis, G. (2002). Assessment of crop damage using space remote sensing and gis. *International Journal of Remote Sensing*, 23(3):417–427.
- Song, X.-P., Hansen, M. C., Potapov, P., Adusei, B., Pickering, J., Adami, M., Lima, A., Zalles, V., Stehman, S. V., Di Bella, C. M., et al. (2021). Massive soybean expansion in south america since 2000 and implications for conservation. *Nature sustainability*, 4(9):784–792.
- Stewart, A., Lehmann, N., Corley, I., Wang, Y., Chang, Y.-C., Ait Ali Braham, N., Sehgal, S., Robinson, C., and Banerjee, A. (2024). SSL4EO-L: Datasets and foundation models for Landsat imagery. *Advances in Neural Information Processing Systems*, 36.
- Stewart, A. J., Robinson, C., Corley, I. A., Ortiz, A., Lavista Ferres, J. M., and Banerjee, A. (2022). TorchGeo: Deep learning with geospatial data. In *Proceedings of the 30th International Conference on Advances in Geographic Information Systems, SIGSPATIAL '22*, pages 1–12, Seattle, Washington. Association for Computing Machinery.
- Tang, P., Chanussot, J., Guo, S., Zhang, W., Qie, L., Zhang, P., Fang, H., and Du, P. (2024). Deep learning with multi-scale temporal hybrid structure for robust crop mapping. *ISPRS Journal of Photogrammetry and Remote Sensing*, 209:117–132.
- Tseng, G., Zvonkov, I., Nakalembe, C., and Kerner, H. R. (2021). Cropharvest: A global dataset for crop-type classification. In *NeurIPS Datasets and Benchmarks*.
- USDA NASS (2024). Cropland data layer. USDA NASS Marketing and Information Services Office.
- Van Klompenburg, T., Kassahun, A., and Catal, C. (2020). Crop yield prediction using machine learning: A systematic literature review. *Computers and Electronics in Agriculture*, 177:105709.
- Verhegghen, A., d’Andrimont, R., Waldner, F., and Van der Velde, M. (2021). Accuracy assessment of the first eu-wide crop type map with lucas data. In *2021 IEEE International Geoscience and Remote Sensing Symposium IGARSS*, pages 1990–1993.
- Wang, Y., Braham, N. A. A., Xiong, Z., Liu, C., Albrecht, C. M., and Zhu, X. (2023). Ssl4eo-s12: A large-scale multimodal, multitemporal dataset for self-supervised learning in earth observation [software and data sets]. *IEEE Geoscience and Remote Sensing Magazine*, 11:98–106.
- Western Cape Department of Agriculture and Radiant Earth Foundation (2021). Crop type classification dataset for western cape, south africa. Radiant MLHub. Version 1.0.
- You, N., Dong, J., Huang, J., Du, G., Zhang, G., He, Y., Yang, T., Di, Y., and Xiao, X. (2021). The 10-m crop type maps in northeast china during 2017–2019. *Scientific data*, 8(1):41.
- Yuan, Y., Lin, L., Zhou, Z.-G., Jiang, H., and Liu, Q. (2023). Bridging optical and sar satellite image time series via contrastive feature extraction for crop classification. *ISPRS Journal of Photogrammetry and Remote Sensing*, 195:222–232.

## A Appendices

### A.1 Data and Materials

All code used to reproduce the results of this paper are distributed on GitHub under the Apache-2.0 license, and all data and model weights are distributed on Hugging Face under the CC-BY-SA-4.0 license. URLs for GitHub and Hugging Face will be released in October.

## A.2 Class Mapping

Table 4 contains the mapping used to convert the original raw datasets to our harmonized class labels. For CDL, double cropping is converted to no data because it could confuse the model during training. Setting them to no data can make them be ignored during training. In datasets like CDL and EuroCrops, subclasses like durum wheat, spring wheat, and winter wheat are harmonized into a single “wheat” class. For EuroCrops, SACT, and AgriFieldNet, “nodata” pixels are taken to be fields without any labels. Note that NCCM, SAS, SACT, and AgriFieldNet are missing crop classes for one or more cereal crops. These crops may or may not appear in the “other” class, resulting in decreased model performance. Better crop type maps are needed for these regions.

Table 4: Class mapping linking the original datasets we chose with our harmonized class labels.

Crop Type	Harmonized	CDL	NCCM	SAS	EuroCrops	SACT	AgriFieldNet
No data	0	0, 225–226, 228, 230–241	15	N/A	No field polygon	0	0
Maize	1	1, 12–13	1	N/A	33010106**	N/A	9
Soybean	2	5	2	1	330116****	N/A	N/A
Rice	3	3	0	N/A	33010107**	N/A	36
Wheat	4	22–24	N/A	N/A	33010101**, 33010102**	7	1
Other	5	Others	3	0	Others	Others	Others

## A.3 Class Distribution

Table 5 lists the total number of pixels belonging to each class after subsampling the dataset to only 1,000 images. Figure 4 displays this same class distribution as a bar chart. Note that certain classes like rice only show up in a few regions. Also note that due to the scarcity of labeled fields in NCCM, the majority of pixels in the dataset are “nodata”.

Table 5: Class distribution of the harmonized global crop type dataset (number of pixels).

Dataset	Maize	Soybean	Rice	Wheat	Other
CDL	8,992,494	7,958,444	0	4,204,954	44,143,414
NCCM	9,417,948	3,955,517	2,890,754	0	48,861,366
EuroCrops	1,759,553	192,698	3,970,909	7,721,286	27,418,993
AgriFieldNet	7,881	0	2,881	63,326	85,872
SAS	0	22,348,399	0	0	43,187,601
SACT	0	0	0	6,049,292	19,065,379

## A.4 Extended Metrics

Figure 5 displays additional evaluation metrics for all in-distribution (ID) and out-of-distribution (OOD) experiments. Due to class imbalance, the average metrics (computed over each class and then averaged) tend to be lower than the overall metrics (computed over all pixels independent of class). Most regions improve the performance metrics with more ID data. However, AgriFieldNet (OOD + ID) diverges from the pattern of improving performance metrics due to the sparsity of labels in the dataset.

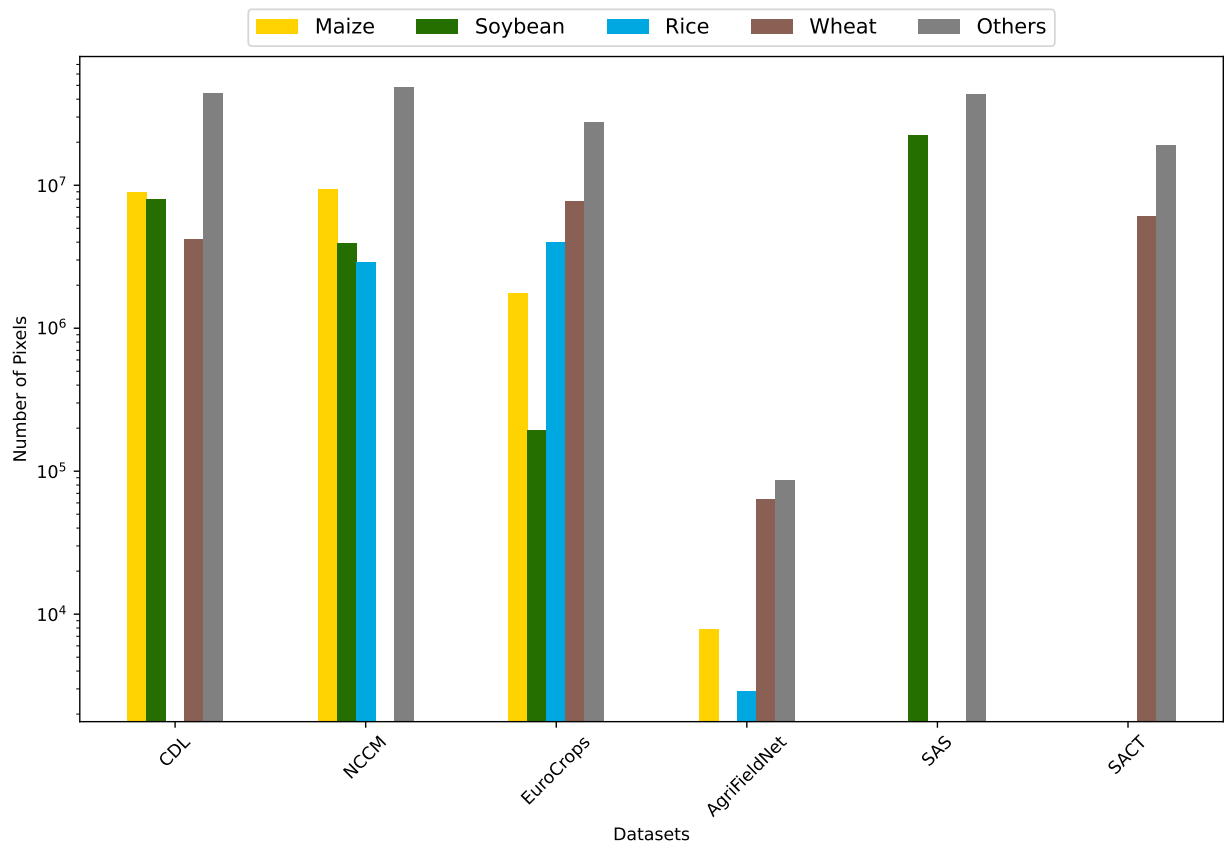


Figure 4: Class distribution for all regions after subsampling.

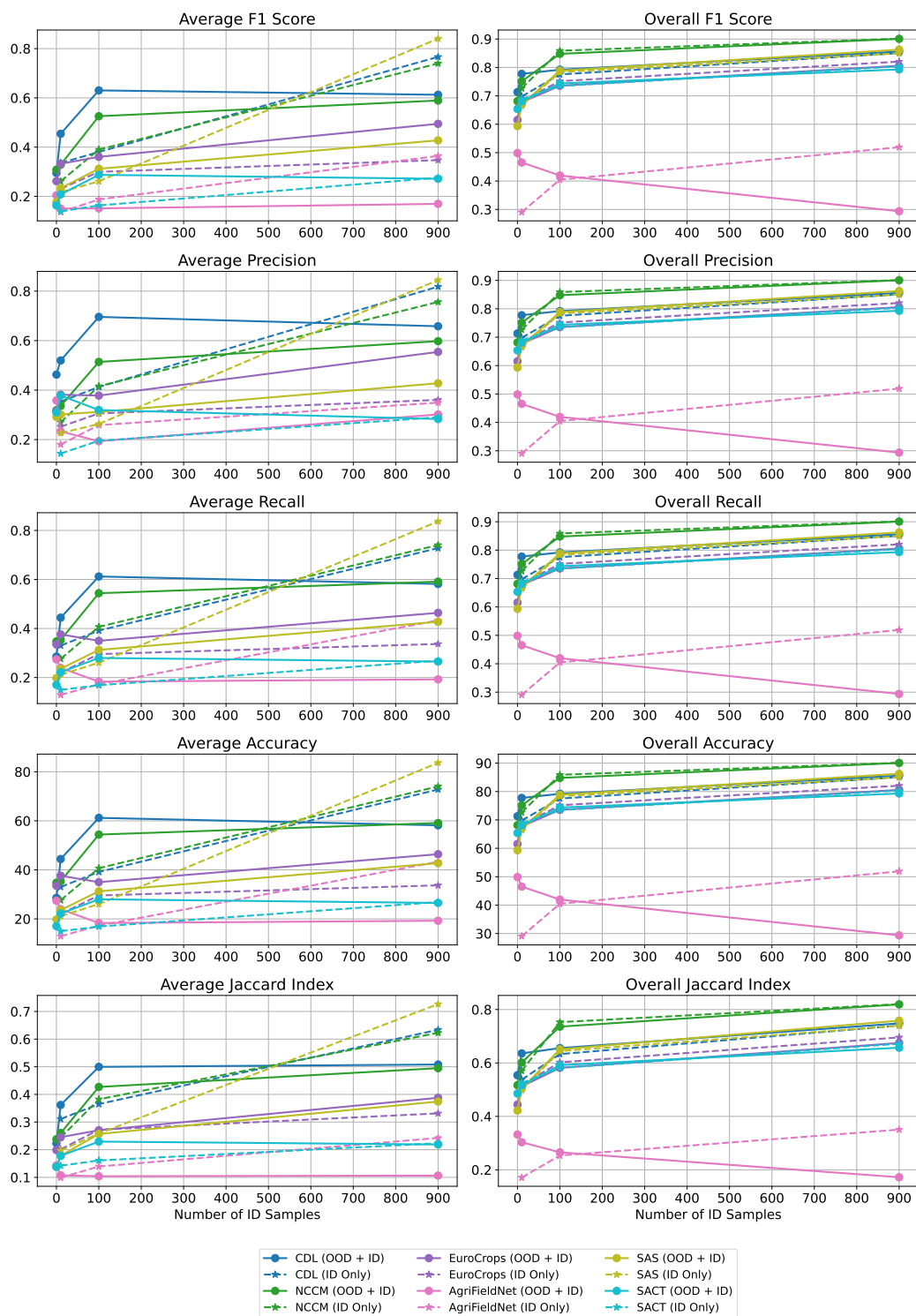


Figure 5: Metrics of ID and OOD + ID. Average and overall metrics are given for F1-score, precision, recall, accuracy, and jaccard index (IoU). For all metrics, higher is better.